



Meshfree CAD-CAE Integration through Immersed B-rep model and Enriched Isogeometric Analysis

Yaxiong Chen¹ , Chetan Jois²  and Ganesh Subbarayan³ 

¹Purdue University, chen2018@purdue.edu

²Purdue University, cjois@purdue.edu

³Purdue University, ganeshs@purdue.edu

Corresponding author: Ganesh Subbarayan, ganeshs@purdue.edu

Abstract. The goal of the present study is to develop techniques to enable CAE-CAE integration by immersing B-rep CAD models within a spatial analysis grid. The developed method relies on point classification and enforcing boundary conditions using signed algebraic level sets and Enriched Isogeometric Analysis (EIGA) respectively. In EIGA, the boundaries as well interfaces are explicitly represented by lower-dimensional spline entities with degrees of freedom corresponding to the enrichment directly specified on the control points of the boundary. The field approximations of the underlying domain are enriched with the boundary conditions and blended with domain field using distance from the boundary. Signed algebraic distance field is used as a measure of distance and the point classification problem is solved as a by-product. The analysis is carried out directly on the B-rep surfaces created by the CAD software without further generating volumetric discretization. We demonstrate good convergence behavior of the proposed method through a patch test. Several numerical examples are included as a demonstration of the method.

Keywords: CAD-CAE integration, Isogeometric analysis, B-rep model, Boundary condition
DOI: <https://doi.org/10.14733/cadaps.2020.1193-1214>

1 INTRODUCTION

In engineering analysis, the task of Computer Aided Design (CAD) is to accurately capture the geometry of the modeled objects, while the task for Computer Aided Engineering (CAE) is to estimate numerical solutions to the partial differential equations (PDEs) that govern the behavior. Historically, the two phases of engineering analysis used different mathematical representations. Most CAD systems adopt Non-Uniform Rational B-Spline (NURBS) representation, while CAE commonly employs Lagrangian interpolations that are central to finite element analysis. Therefore, using identical mathematical representation for geometry and behavior would enable efficient CAD-CAE integration. Building behavioral approximations using the same parametric

spline basis as geometry was proposed early by the corresponding author among others [6, 18, 9, 14]. The use of such approximations for analysis is at present popularly referred as Isogeometric Analysis (IGA, [7]).

Currently, most CAD systems utilize boundary representation (B-rep) models constructed from trimmed Non-Uniform Rational B-Splines (NURBS) patches. The IGA models, on the other hand, commonly assume the availability of volumetric tensor product splines that ‘mesh’ the domain. The mesh generation process typically replaces the original B-rep model with a volumetric spline representation [31, 30, 1]. In this sense, volumetric discretization in IGA plays the same role as mesh generation in finite element analysis. Thus, although the original motivation of IGA is to narrow the gap between CAD and CAE, in practice, considerable intermediate steps remain between B-rep CAD models and analysis suitable IGA models.

An alternative approach to constructing analysis suitable tri-variate splines is to immerse the B-rep model within a regular grid in space containing analysis unknowns. This idea originates from the finite element community and is called immersed boundary method [16] (or finite cell method, fictitious domain method, embedded domain method). The fundamental strategy is to extend the physical domain of interest beyond its complex parametric boundaries into a larger embedding domain of a simpler geometry, thus allowing for a simpler structured grid. In the immersed boundary method, the mesh does not conform to the B-rep model boundary. The challenge of generating analysis suitable mesh is converted to one of accurately representing the physical fields and carrying out numerical quadrature precisely in the immersed domain.

When the analysis grid does not conform to the B-rep model boundary, no behavioral degree of freedom exists directly on the essential boundary of the physical domain for one to apply the boundary condition directly. This challenge, common to nearly all meshfree approximations including moving least square [11] and reproducing kernel [10] methods, necessitates weak imposition of boundary conditions through one of many possible techniques including the penalty functions [32], Lagrange multipliers method [2], Augmented Lagrangian [29], or Nitsche’s method [8]. The challenge of applying boundary conditions is not restricted to immersed boundaries, but also exists when volumetric NURBS patches are used for analysis since the behavioral degrees of freedom are associated with the control points and not the geometrical boundary. Similar to other mesh free method basis functions, the NURBS basis does not interpolate the control or nodal points. The non-interpolatory nature of the basis functions necessitates the earlier mentioned approaches to the application of the essential boundary conditions.

When immersing boundary representation model in the underling domain, it is necessary to determine whether a quadrature point in the regular grid is inside or outside the geometrical domain. The most commonly used method for point membership classification is ray tracing [20, 19]. Any point inside the solid model intersects the surface of the model an odd number of times. This kind of operation is usually computationally intensive. Therefore, a more efficient point member classification is necessary for immersed boundary solutions.

In general, direct application of boundary condition is an issue for mesh free approximation of fields, specifically, immersed boundary method. Furthermore, the point classification is tedious and computational expensive. Both task are not efficiently addressed in prior literature. So they are the goal of this paper.

In the present paper, we proposed a new approach to analyze complex B-rep models immersed in regular grids. We constructed the specific form for direct application of boundary condition based on Enriched Isogeometric Analysis (EIGA [25]). In EIGA, the boundaries as well interfaces are explicitly represented by lower-dimensional NURBS entities with additional degrees of freedom directly specified on the control points of the interface geometry. Furthermore, the field approximation on the continuous domain is enriched with an approximation with known characteristics defined on the enriching boundaries. For instance, the enriching boundary may correspond to a crack, in which case the enrichment must possess the known physical behavior such as displacement discontinuity on the boundary. The influence of any enrichment, behavioral or otherwise, is generally expected to decrease with distance (see for instance heterogeneous material modeling using distance fields [5]). Thus, the composition of the enriching boundary is restricted to a local region as dictated by a weight function that varies monotonically with respect to distance from the boundary. In our prior work, a monotonic measure of approximate distance was constructed using algebraic level sets [27, 28]. Furthermore,

the sign of the algebraic level sets constructed on bounded solids enables the point membership query for CAD/CAE applications.

The organization of the paper is as follows. In Section 2, we introduce Enriched Isogeometric Analysis and discuss application of boundary conditions as an enrichment. In Section 3, we introduce the concept of algebraic level sets and describe point membership classification using signed algebraic level sets. Several numerical examples are illustrated in Section 4 to demonstrate the meshfree CAD-CAE integration. The paper is summarized in Section 5.

2 BOUNDARY CONDITION APPLICATION

In the original description of isogeometric analysis [7], the essential boundary conditions were directly applied to the control variables. We refer to this approach as direct imposition of Dirichlet boundary conditions. A direct application of boundary conditions on control points is reasonable if control points don't coincide with points of application of the essential boundary condition on the domain.

In the immersed boundary method, the essential boundary conditions are often applied using a weak form, in which the integral of the displacement constraint on the boundary is set to zero. That is, the constraint is enforced in an averaged sense than point by point. The weak form constraint is most commonly enforced using Lagrange multipliers [2]. However, the use of Lagrange multipliers to enforce the constraint may cause the solution matrix system to lose its positive definiteness. On the other hand, the penalty method [32] and Nitsche's method [8] require only the selection of one scalar parameter. In the penalty method, the selected parameter must be large enough to ensure the accurate enforcement of the essential boundary conditions, while too large a value leads to ill-conditioned system of equations. In comparison, Nitsche's method does not suffer from ill-conditioning. However, an empirical stabilization parameter is needed, so the implementation of Nitsche's method is not as trivial as the Lagrange multiplier method or the penalty method; the choice of the stabilization parameter will depend on the problem at hand. In this paper, we propose a new method to apply boundary conditions based on the theory of Enriched Isogeometric Analysis (EIGA). In EIGA, the boundaries are treated as lower-dimensional enrichments. Extra degrees of freedom are added to the control points of the boundary. The field approximation on the domain is enriched with an approximation near the enriching boundaries through a blending function. The method also allows the direct application of the boundary condition on the enrichment.

2.1 Enriched Isogeometric Analysis

The concept of enriched field approximations is enabled by Partition of Unity Finite Element Method (PUFEM) [12] and the Generalized Finite Element Method (GFEM) [24]. In GFEM, the underlying finite element approximation is generalized by adding degrees of freedom representing complex local behavior. Convergence of the approximations is ensured by the partition of unity property of the finite element shape functions. In other words, the FE approximation space is "enriched" by the known local behavior. As demonstrated by Strouboulis [24], the concept of GFEM can be applied to problems with known behaviors including boundary conditions, displacement discontinuity at a crack face, and asymptotic behavior near reentrant corners.

Tambat and Subbarayan [25] proposed the so called Enriched Isogeometric Analysis wherein they enriched known behavior on the explicitly defined lower-dimensional geometric features. The base approximations are "enriched" isogeometrically on parametrically defined lower-dimensional geometrical features and by constructing distance fields from them. Both the underlying domain and the lower-dimensional geometry are represented by Non-Uniform Rational B-Splines (NURBS). The EIGA blending function for an arbitrary field is

$$f(x) = (1 - \sum_{i=1}^{n_e} w_i) f_{\Omega}(x) + \sum_{i=1}^{n_e} w_i f_{\Gamma_i}(\mathcal{P}(x)) \quad (1)$$

where, Ω is the underlying domain and f_Ω is the associated continuous field, Γ_i is the i^{th} lower dimensional geometry (internal/external boundary) with f_{Γ_i} being the corresponding enriching approximation. To compute f_{Γ_i} at a spatial point \mathbf{x} in Ω , it is necessary to project the point onto the boundary $\mathbf{u}_f = \mathcal{P}(\mathbf{x})$ to map \mathbf{x} to the parametric space of the lower-dimensional geometry $C(\mathbf{u})$. A general illustration of EIGA with single enrichment is shown in Fig. 1. w_i is the weight function, which represents the contribution of i^{th} enrichment

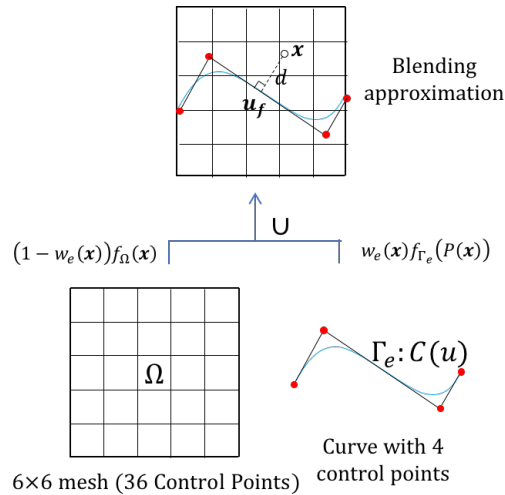


Figure 1: Graphical illustration of constructing Enriched Isogeometric approximation.

to the blending function. It is a monotonically decreasing function of distance. There are multiple choices for the form of $w(d)$ including exponential, cubic and quartic among others, but they must satisfy the following conditions:

1. Value is 1 on the enrichment and 0 outside the domain of influence.
2. Derivative is 0 on the enriching curve and at the edge of the domain of influence.

The weight functions used in the present paper are listed below and illustrated in Fig.1:

Cubic

$$w(\bar{d}) = \begin{cases} 1 - 3\bar{d}^2 + 2\bar{d}^3 & 0 \leq \bar{d} < 1 \\ 0 & \bar{d} \geq 1 \end{cases} \quad (2)$$

Quartic

$$w(\bar{d}) = \begin{cases} 1 - 6\bar{d}^2 + 8\bar{d}^3 - 3\bar{d}^4 & 0 \leq \bar{d} < 1 \\ 0 & \bar{d} \geq 1 \end{cases} \quad (3)$$

Exponential [3]

$$w(\bar{d}) = \begin{cases} 1 - \frac{1 - e^{-(\bar{d}/\alpha)^p}}{1 - e^{-[1/\alpha]^p}} & 0 \leq \bar{d} < 1 \\ 0 & \bar{d} \geq 1 \end{cases} \quad (4)$$

where $\bar{d} = d/d_{max}$, d_{max} is the cutoff distance distance of the blending region from the enriching entity.

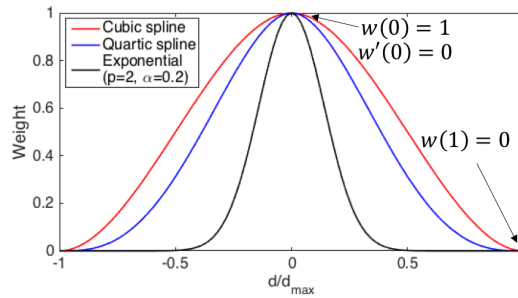


Figure 2: Possible mathematical forms of the weight functions.

2.2 Boundary Conditions as Enrichments

The blending strategy of EIGA can be easily applied to enforce boundary conditions. This is especially useful when a parametric boundary is immersed into a regular analysis grid, since one can apply the boundary conditions directly on the control points of the NURBS geometry rather than weakly enforce them over the surface. To accurately capture the behavior near the boundary, an isogeometric approximation with hybrid function/derivative enrichment is proposed in the present paper. This enriched approximation is a smooth blending of C^1 or higher order continuous isogeometric approximation of underlying domain enriched with a C^0 continuous local approximation. Eq. (5) illustrates the mathematical form of the enrichment and its associated extra degrees of freedom.

$$\mathbf{u}(x) = (1 - w^e(d))\mathbf{u}^c(x) + w^e(d) * (\mathbf{u}^e(\mathcal{P}(x)) + d * \mathbf{G}^e(\mathcal{P}(x))) \tag{5}$$

The \mathbf{u}^c term in Eq. (5) corresponds to the contribution of the approximation in the underlying domain, while the second part is from the enrichment. \mathbf{u}^e represents the motion of the boundary while \mathbf{G}^e represents the normal derivative of the displacement on the enrichment. The discretization of \mathbf{u}^c , \mathbf{u}^e and \mathbf{G}^e are as follows:

$$\mathbf{u}^c = \sum_{n=1}^{n^c} \mathbf{N}_i^c \mathbf{u}_i^c \tag{6}$$

$$\mathbf{u}^e = \sum_{n=1}^{n^e} \mathbf{N}_i^e \mathbf{u}_i^e \tag{7}$$

$$\mathbf{G}^e = \sum_{n=1}^{n^e} \mathbf{N}_i^e \mathbf{G}_i^e \tag{8}$$

where, \mathbf{u}^c , \mathbf{u}^e , \mathbf{G}^e are the fields to be solved, and \mathbf{u}_i^c , \mathbf{u}_i^e , \mathbf{G}_i^e are the discrete unknown values at the i^{th} control point, N_i^c and N_i^e are the rational NURBS basis functions corresponding to the underlying domain and the boundary respectively.

The matrix form of Eq. (5) is:

$$\mathbf{u} = \begin{bmatrix} (1 - W^e)\mathbf{N}^c & W^e N^e & W^e d N^e \end{bmatrix} \begin{Bmatrix} u^c \\ u^e \\ G^e \end{Bmatrix} \tag{9}$$

The corresponding strain field is

$$\varepsilon = \nabla_s \mathbf{u} = [\mathbf{B}] \{ \mathbf{u} \} \quad (10)$$

with

$$\nabla_s = \begin{bmatrix} \frac{\partial}{\partial x} & 0 \\ 0 & \frac{\partial}{\partial y} \\ \frac{\partial}{\partial y} & \frac{\partial}{\partial x} \end{bmatrix} \quad (11)$$

$$[\mathbf{B}] = [B^c \quad B^e \quad B^G] \quad (12)$$

where

$$\begin{aligned} B^c &= (1 - w^e) \nabla_s N^c - \nabla_s w^e N^c \\ B^e &= \nabla_s w^e N^e + w^e \nabla_s N^e \\ B^G &= \nabla_s d w^e N^e + d \nabla_s w^e N^e + d w^e \nabla_s N^e \end{aligned} \quad (13)$$

The linear equation system resulting from the discretization that needs to be solved has the form:

$$\begin{bmatrix} K^{cc} & K^{ce} & K^{cG} \\ K^{ec} & K^{ee} & 0 \\ K^{Gc} & 0 & K^{GG} \end{bmatrix} \begin{Bmatrix} \mathbf{u}_c \\ \mathbf{u}_e \\ \mathbf{G} \end{Bmatrix} = \begin{Bmatrix} 0 \\ \mathbf{f}_e \\ 0 \end{Bmatrix} \quad (14)$$

where,

$$[K^{IJ}] = \int_{\Omega} B^{IT} D B^J d\Omega \quad (15)$$

with I, J representing *c*, *e* and *G*.

2.3 Dirichlet Boundary Conditions

In the immersed boundary method, the boundary in general does not coincide with the edge of the element. In the present study, the Dirichlet boundary conditions are enforced point-wise on the enrichment boundary as described below. The boundary is represented by a closed curve Γ , the Dirichlet and Neumann boundary condition are applied on part of Γ , which are marked as Γ_d and Γ_n in Fig. 3. To apply the boundary condition, Γ_d and Γ_n are extracted from the B-rep CAD model and reparametrized as two NURBS entities $\Gamma_d(t)$ and $\Gamma_n(t)$ varying with parameter t . The boundary conditions are now applied on the control points of the above NURBS entities.

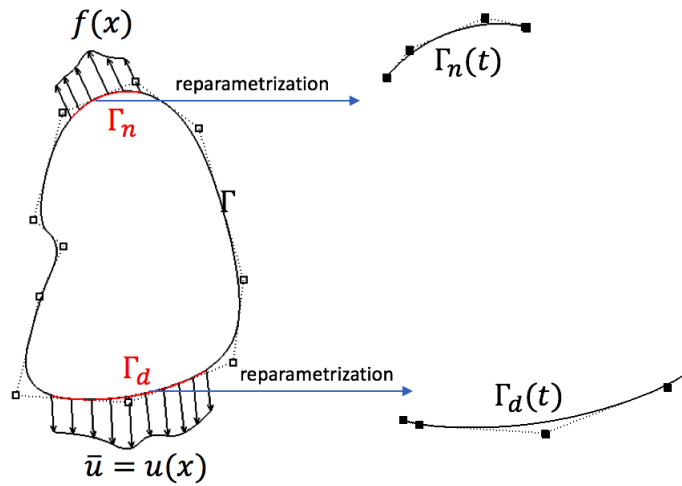


Figure 3: Boundary reparametrization (The subregions of the boundary where Dirichlet or Neumann conditions are applied are extracted and reparametrized so boundary conditions may be directly imposed on the newly generated control points).

The homogeneous boundary conditions ($\mathbf{u}^e = 0$) can be easily applied by setting $\mathbf{u}_i^e = 0$ in Eq. (7). Similarly, if the value of Dirichlet boundary conditions is a non-zero constant, every \mathbf{u}_i^e in Eq. (7) is set to the constant value; the partition of unity property of the basis function will ensure a constant displacement on the whole enrichment boundary. In the general case of inhomogeneous Dirichlet boundary condition, the varying value may only be enforced approximately. In the present study, a least squares solution is used to determine the value \mathbf{u}_i to be enforced on each control point of the Dirichlet boundary. Let the distribution of the displacement vector field $\mathbf{u}(\mathbf{x})$ on the boundary be of an arbitrary form $\mathbf{u}(\mathbf{x}(t))$, where, t is the parametric description of the reparametrized region Γ_d , on which the condition is applied, and \mathbf{x} are the cartesian coordinates corresponding to the parametric location. The problem now is to minimize the function:

$$f(\mathbf{u}_i) = \int \left[\mathbf{u}(\mathbf{x}(t)) - \sum_{i=0}^n N_i(t) \mathbf{u}_i \right]^2 dt \quad (16)$$

and the optimality condition is:

$$\frac{\partial f}{\partial \mathbf{u}_j} = -2 \int N_j \left[\mathbf{u}(t) - \sum_{i=0}^n N_i^T(t) \mathbf{u}_i \right] dt = 0 \quad (17)$$

This will yield the following linear system for the unknown control point values of the vector \mathbf{u}_i :

$$\left[\int N_j(t) N_i^T(t) dt \right] \mathbf{u}_i = \int N_j \mathbf{u}(t) dt \quad (18)$$

The solution to the linear system is then enforced as the appropriate control point quantities \mathbf{u}^e in Eq. (7).

2.4 Neumann Boundary Conditions

Let the distributed load on the boundary be of the form $\mathbf{f}(\mathbf{x})$ applied on the reparametrized region Γ_n on which the Neumann condition is applied, and \mathbf{x} is the physical coordinate. Here, we seek a work equivalent

force \mathbf{f}_i of the form:

$$\int \mathbf{f}(\mathbf{x})\delta\mathbf{u}d\mathbf{x} = \sum_i \mathbf{f}_i\delta\mathbf{u}_i \tag{19}$$

where, $\delta\mathbf{u}(\mathbf{x})$ is a virtual displacement applied on the boundary Γ_n , and $\delta\mathbf{u}_i$ are the control point values of the discretized virtual displacement $\delta\mathbf{u}(\mathbf{x})$. The control points here correspond to the reparametrized curve shown in Fig. 3. Since a work equivalent force is to be defined on the control points of the boundary surface parametrized by t , a change of variables from \mathbf{x} to t is necessary to apply the Neumann condition

$$\mathbf{f}_i = \int N_i(\mathbf{x})\mathbf{f}(\mathbf{x})d\mathbf{x} = \int N_i(t)\mathbf{f}(\mathbf{x}(t))\left|\frac{d\mathbf{x}}{dt}\right|dt = \int N_i\mathbf{f}(t)|J|dt \tag{20}$$

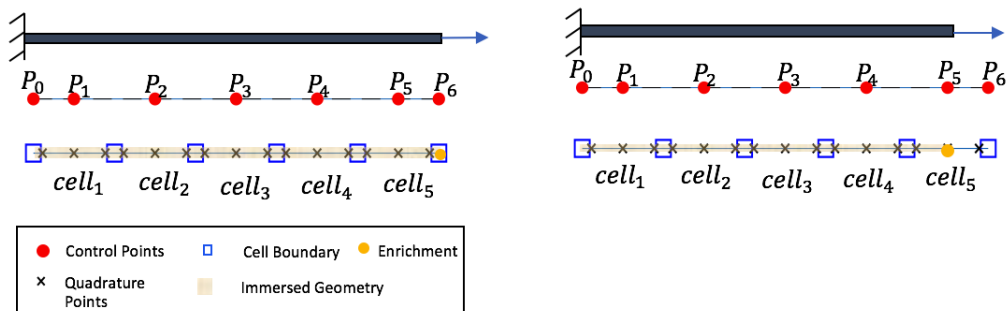
where, J is the Jacobian associated with the variable change:

$$J_{pq} = \frac{\partial x_p}{\partial t_q} \tag{21}$$

where, x_p is the p^{th} component of \mathbf{x} . This is very similar to Neumann boundary application in FEM, where equivalent force is applied on the corresponding nodes on the Neumann boundary. Using Eq. (20), the value of \mathbf{f}^e is enforced in Eq. (14).

2.5 Illustration with a One-Dimensional Example

To illustrate the boundary condition application, as shown in Fig. 4, a one-dimensional bar under tension is immersed in either a domain fitting discretization (conforming boundary) or in a larger domain (non-conforming boundary). In this problem, the two end points of the bar represent the boundary. The bar is immersed in a background B-spline mesh. The background is discretized into 5 knot spans using 7 control points. The corresponding basis functions are shown in Fig. 5, where $N_{i,2}$ refers to the i^{th} basis function of degree 2. When the immersed geometry conforms to the background discretization, homogeneous Dirichlet boundary condition at point P_0 is enforced by constraining the end control point P_0 . The Neumann boundary condition, on the other hand, is applied as an enrichment.



(a) Case 1: Immersed domain conforming to background discretization.

(b) Case 2: Immersed domain not conforming to background discretization.

Figure 4: A one-dimensional immersed boundary example.

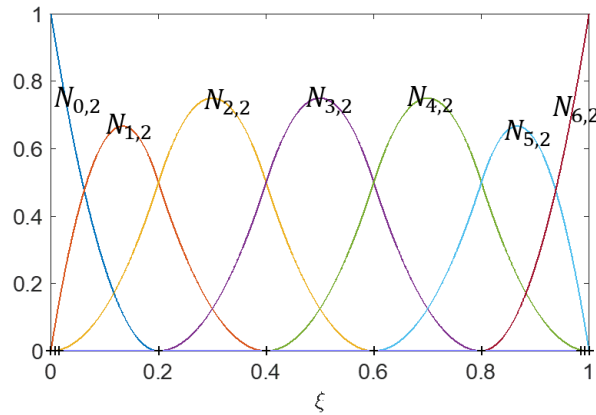


Figure 5: B-spline basis functions of the background domain.

In the first case, the enrichment is conformal with the boundary of the cell (Fig. 4a). The location of the enrichment is coincident with control point P_6 . Two degrees of freedom, u^e and u^G associated with the enrichment will now be added to the system. We can then rewrite Eq. (9) as

$$\mathbf{u} = \begin{bmatrix} \hat{\mathbf{N}}_i & \hat{N}_e & \hat{N}_G \end{bmatrix} \begin{Bmatrix} u^c \\ u^e \\ G^e \end{Bmatrix} \quad (22)$$

where, $\hat{\mathbf{N}}_i = (1 - W^e)\mathbf{N}_i^c$, $\hat{N}_e = W^e N^e$, $\hat{N}_G = W^e N^e d$ are the modified basis functions corresponding to each degree of freedom. The influence of enrichment does not extend outside of $cell_5$. Therefore, the influence of N_e and N_G also do not extend outside of $cell_5$. Due to the blending of the enrichment, the basis functions N_4 , N_5 , and N_6 in $cell_5$ are modified as shown in Fig. 6a.

In the second case, the immersed domain does not conform to the background discretization as shown in Fig. 4b. The right end of the immersed bar is located in the middle of $cell_5$. In this case, it is not possible to apply the boundary condition directly on the end control point. The underlying domain is now enriched at the end point of the immersed bar. The basis function value at points outside the immersed domain are set to equal to zero as shown in Fig. 6b. In this example, the blending region covers both $cell_4$ and $cell_5$, and so N_3 to N_6 require to be modified in the immersed domain. The modification ensures that the partition of unity property still holds.

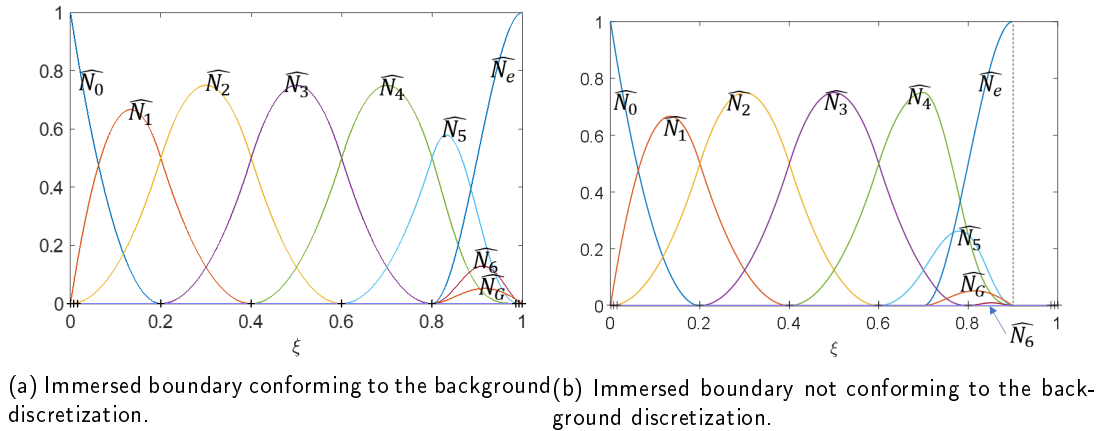


Figure 6: Basis functions of the enriched approximations.

2.6 Patch Test

To validate the developed method, a ‘patch’ test for both Dirichlet and Neumann conditions is conducted. The patch test is intended to verify that the blended numerical approximation is able to reproduce uniform displacement derivative or stress values. The chosen immersed region is of size 1×1 with a Young’s modulus value of 1 and Poisson’s ratio of 0.3. The bottom edge is fixed and the top edge is under tension as shown in Fig. 7. A homogeneous Dirichlet condition is applied at the bottom. On the top, a Dirichlet condition of constant displacement $u_y = 1$ (Fig. 8a) or a Neumann condition of uniform stress of $f_y = 1$ (Fig. 8b) are applied. The patch is immersed in a B-spline discretization with regularly spaced control points. A convergence study is also conducted with different cell sizes. Elasticity theory dictates identical solution with a linearly varying displacement in the vertical direction in both cases.

In the study, two error norms - energy norm (Eq. (23)) and displacement norm (Eq. (24)) - are defined to measure the error between the exact solution and numerical solution. In addition, the influence of the weight functions listed in Eqs. (2)-(4) are also evaluated.

$$error_e = \left\{ \frac{1}{2} \int (\varepsilon^{num} - \varepsilon^{exact}) : D : (\varepsilon^{num} - \varepsilon^{exact}) d\Omega \right\}^{1/2} \quad (23)$$

$$error_d = \left\{ \int (\mathbf{u}^{num} - \mathbf{u}^{exact}) \cdot (\mathbf{u}^{num} - \mathbf{u}^{exact}) d\Omega \right\}^{1/2} \quad (24)$$

where \mathbf{u}^{num} is the numerical result of displacement and \mathbf{u}^{exact} is the exact solution. Three weight functions (Eqs. (2)-(4)) are compared in the patch test. The blending cutoff distance is chosen to be the size of one cell. The background mesh uses uniform knot spacing on a degree-2 NURBS discretization with a regularly spaced grid of control points. The result for patch test convergence study is shown in Figs. 9 and 10. The cubic and quartic spline weight functions yield solutions that are accurate to machine precision even when coarse mesh is used due the exact integration of polynomials through Gaussian quadrature. Exponential weight function causes less error as cell size decreases.

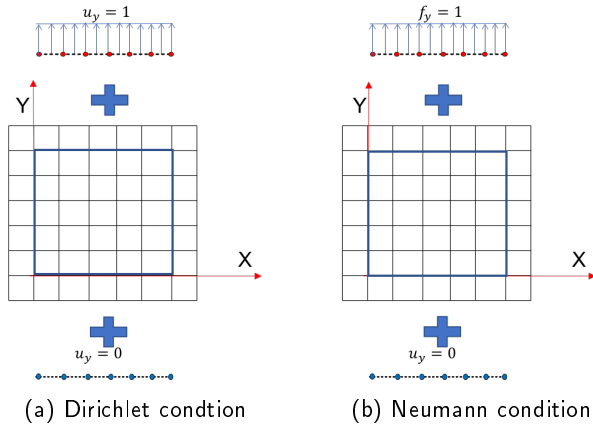
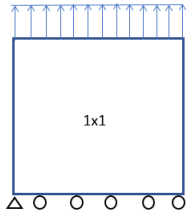


Figure 7: Problem definition: loads and boundary conditions for the patch test.

Figure 8: Illustration of boundary condition application.

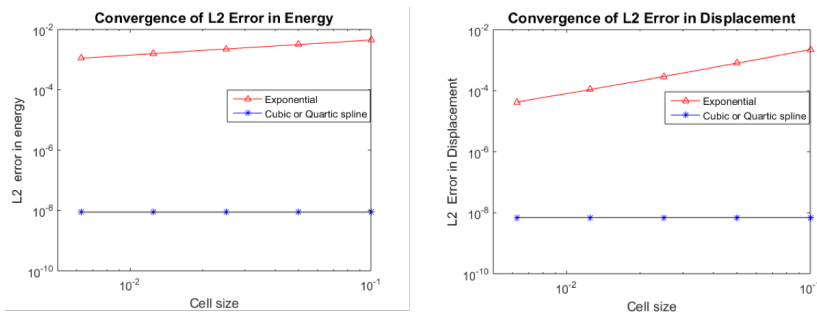


Figure 9: Convergence study for the Dirichlet condition.

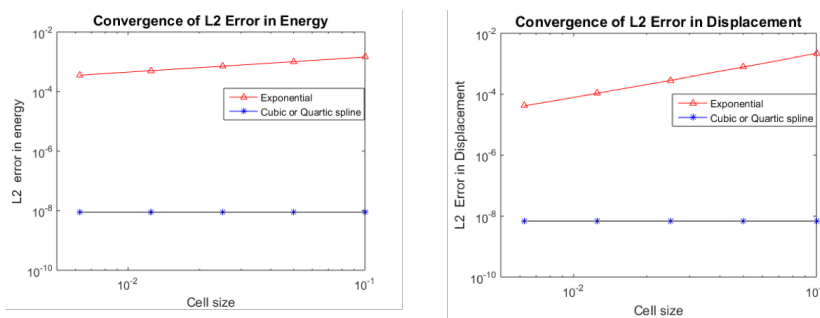


Figure 10: Convergence study for the Neumann condition.

3 SIGNED ALGEBRAIC LEVEL SETS FOR DISTANCE MEASURES

In the last section, we proposed a technique for applying boundary conditions on immersed boundaries (Eq. (5)). In this problem, distance from the boundary or interface serves as a measure of influence of the behavior on the boundary at a point in the underlying domain. Therefore, inexpensive distance calculations from parametric boundaries are critical to the developed procedure. The need for distance measure in the present study is illustrated in Fig. 11. An arbitrary closed boundary is immersed in the spline mesh, with the red crosses representing the quadrature points outside the domain while the blue crosses are quadrature points inside the domain. Γ_d and Γ_n denote the Dirichlet and Neumann boundary.

While the use of Newton-Raphson iterations to estimate distance to a parametric boundary is most common [13, 17], the numerical iterations need to be carried out at every quadrature point. In addition, the Newton-Raphson iterations may also be non-robust in that more than one point on the immersed surface may be equidistant from a quadrature point. An alternative idea is to construct a polytope approximation to the boundary to estimate distance [4, 15]. However, a polytope approximation will not retain the parametric details of the boundary that enables computation of normals and curvatures that are critical to the evolution of the boundary under physical forces. In this study, we build on the recent work of the corresponding author and colleagues [27, 28] to construct signed algebraic level sets that provide both distance measures as well as point classification. The algebraic level sets preserve the exact geometry of low-degree (2 or 3) NURBS curves/surface and avoid iteration. Specifically, in the present study, the algebraic level sets provide a measure of distance to the enrichment at each quadrature point.

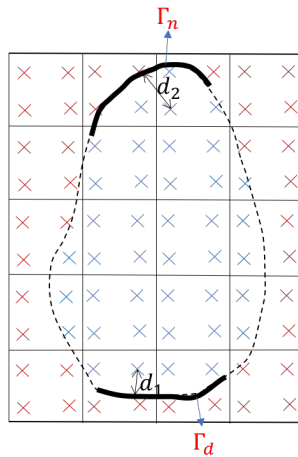


Figure 11: Role of algebraic level sets in CAD-CAE integration.

The main idea behind the algebraic distance field is to implicitize the parametric entity and use the level sets of the implicitized function as a measure of distance. The implicitization of parametric entities is based on the resultant theory, which is described in the seminal research of Sederberg [22]. The resultant of a parametric entity is the determinant of a matrix of the form $\det(\mathbf{M}^B(\mathbf{x})) = 0$, which gives the implicit representation of the parametric entity. Furthermore, for any point \mathbf{x} that is not on the curve, $\Gamma = \det(\mathbf{M}^B(\mathbf{x}))$ is a measure of distance from the curve. Upreti and Subbarayan [27, 28] utilized the resultant to construct signed algebraic level sets. We describe the procedure pictorially in Figs. 12, 13 and 14.

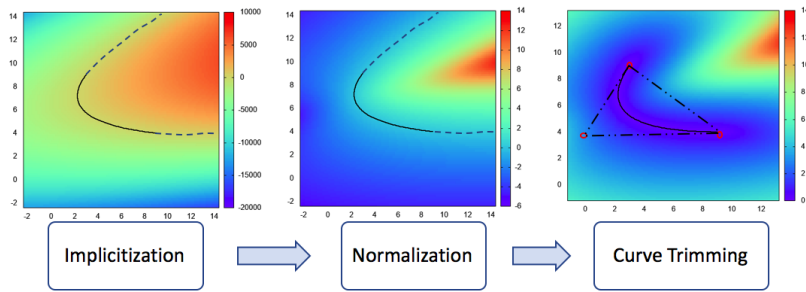


Figure 12: Procedure to construct algebraic distance field for Bezier curves.

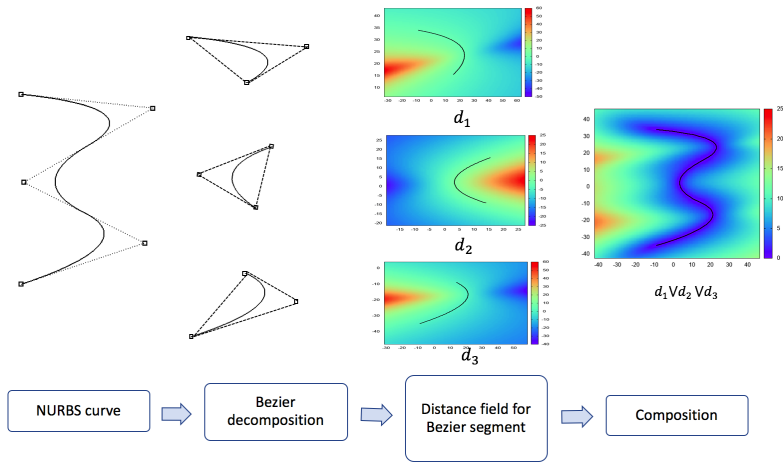


Figure 13: Procedure to construct algebraic distance field for NURBS curves.

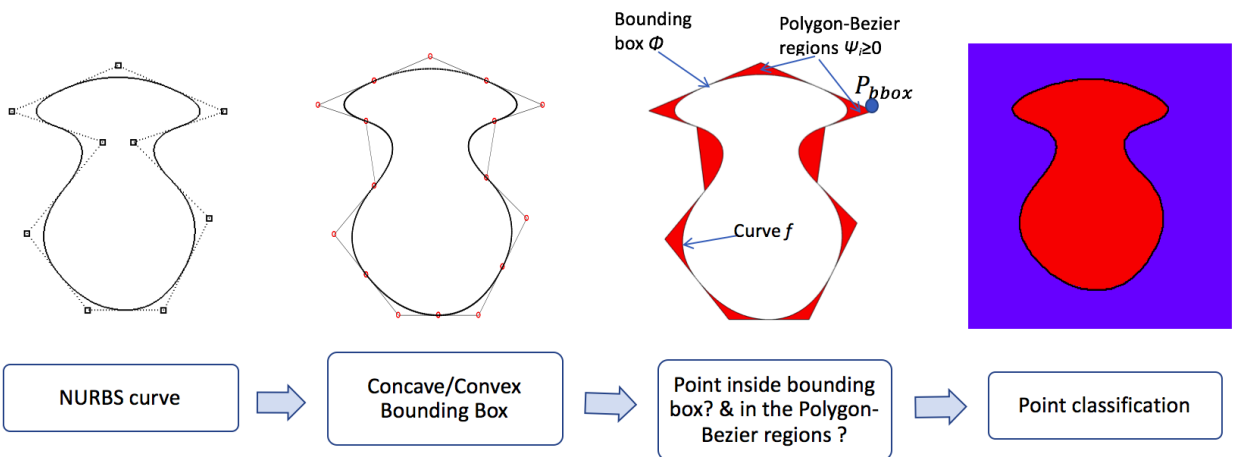


Figure 14: Procedure to construct signed algebraic level sets.

Once the signed algebraic level sets are constructed, the sign is used for point membership classification. For a multiply connected domain, R-functions [23] are used to compose signed algebraic level sets.

4 NUMERICAL EXAMPLES

Fig. 15 describes the general procedure to implement the developed methodology. First, the B-rep model is generated in the CAD system. The geometry of the enriching boundary should also be constructed with the appropriate lower dimensional NURBS representation. This can be done by trimming the B-rep model and extracting the trimmed region where the boundary condition is to be applied. Immersing the B-rep model in the NUBRS background mesh, for each quadrature point, the signed distance field is utilized to classify the point relative to the boundary. If the quadrature point is inside, then the solid's material property is assigned to it. If not, a numerically small value α is used as the elastic modulus so that the contribution of the point is numerically insignificant. M. Ruess et al. [21] point out that for lower order splines, the resulting stiffness matrices are sufficiently well conditioned to allow the application of standard preconditioned iterative solvers. But, for higher order splines, the penalization leads to strongly ill-conditioned matrices that require the application of direct solvers. In our study, we used a direct solver and chose α to be 10^{-6} . The boundary condition is assigned to the corresponding degree of freedom of the enrichment: Dirichlet boundary on u and Neumann on G . The next step is to assemble the system following the procedure outlined in Section 2. Finally, solving the assembled matrix system, we obtain the displacement solution at each control point of the underlying domain. In the following subsections, several numerical examples are illustrated. For simplicity, all parameters are dimensionless, the size of computational region is 1×1 , Young's modulus is 1 and Poisson's ratio is 0.3.

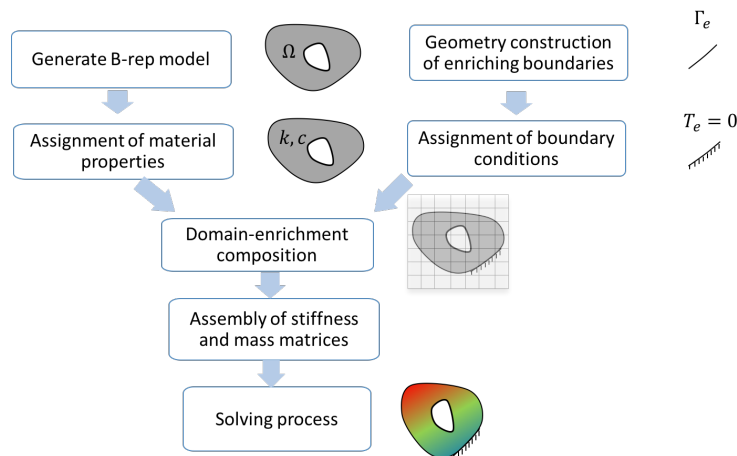


Figure 15: CAD-EIGA integration: flow of control during analysis.

4.1 Plate with a Single Hole

The first example is of a plate with single hole under uniform tension. The geometry, loading, and boundary conditions are described in Fig. 16a and the CAD model is shown in Fig. 16b. The B-rep model is immersed in the NURBS background grid shown in Fig. 16c. In this example, we construct the NURBS grids such that the outer boundary of the CAD geometry conforms to the boundary of the grid cell. Thus, the cells in the brown region lie outside the domain of interest and may be discarded. The algebraic distance field is as shown

in Fig. 16d and the sign of algebraic distance field enables point classification. In Fig. 16e, the red region represents the domain of interest. The weight field shown in Fig. 16f describes the influence of the boundary condition on the underlying domain. The closer the point is to the boundary, the higher its weight. The cutoff distance for the blending region is set to two times of the element size. The Von Mises stress resulting from the analysis is shown in 16g. The results clearly capture the stress concentration in the periphery of the hole.

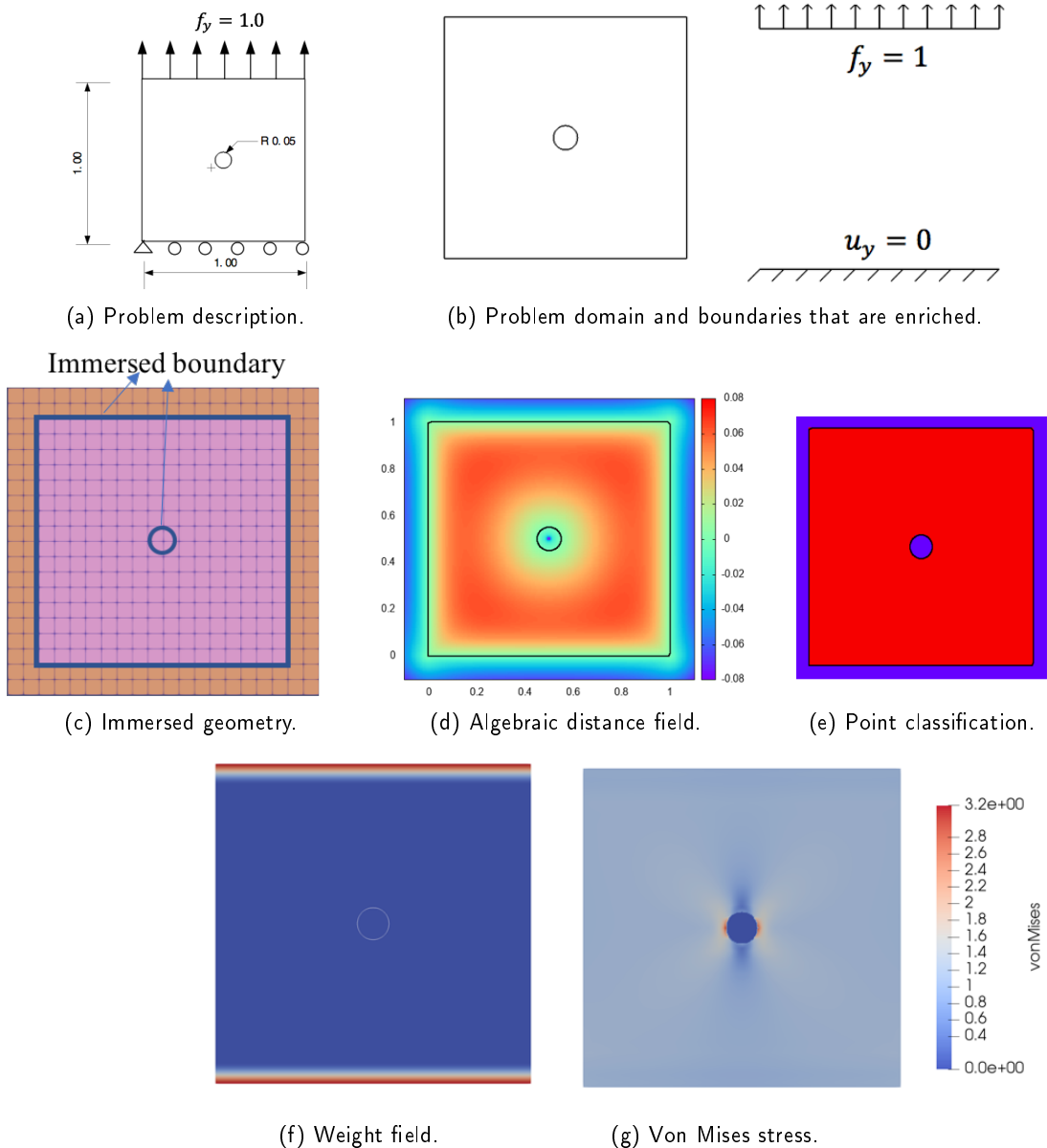


Figure 16: Example 1: Plate with a single hole.

Fig.17a shows the distribution of σ_{22} in the plate. We next carried out a convergence study by varying the

spacing of the background NURBS grid and compared the solution convergence against the known analytical solution for the problem [26]. The stress concentration factor in the plot is defined as $SCF = \frac{\sigma_{max}}{\sigma_{nom}}$, where σ_{nom} is the nominal stress due to a uniform load that one would expect on the section if there were no stress concentration. As can be seen from Fig. 17b, with the decrease of the grid spacing or cell size, the stress concentration factor converges to the analytical result of 2.8.

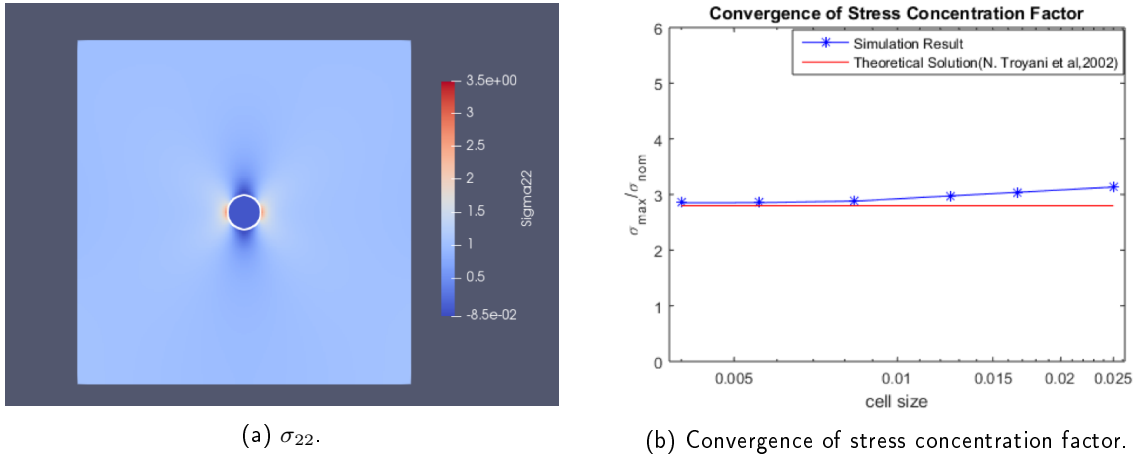


Figure 17: Convergence of σ_{22} .

4.2 Plate with Multiple Holes

This example builds on the first one by increasing the number of holes in the domain. The external geometry, material and boundary conditions are the same as before. Interior to the plate is however different; it now contains nine holes instead of a single one. The details of this example are shown in Fig. 18. The background NURBS grid used is 200×200 . As before, the blending region is twice the grid spacing. Now, each hole causes the stress to concentrate.

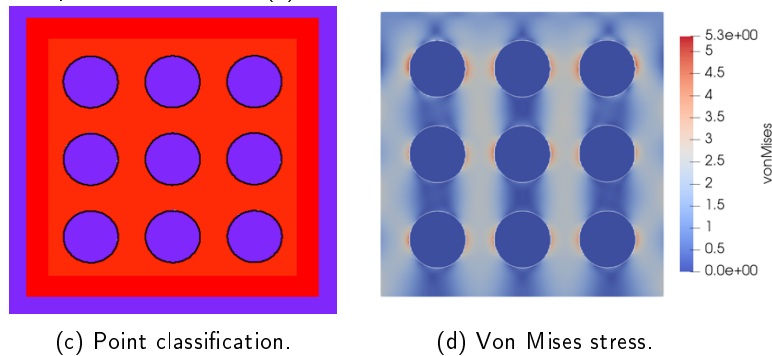
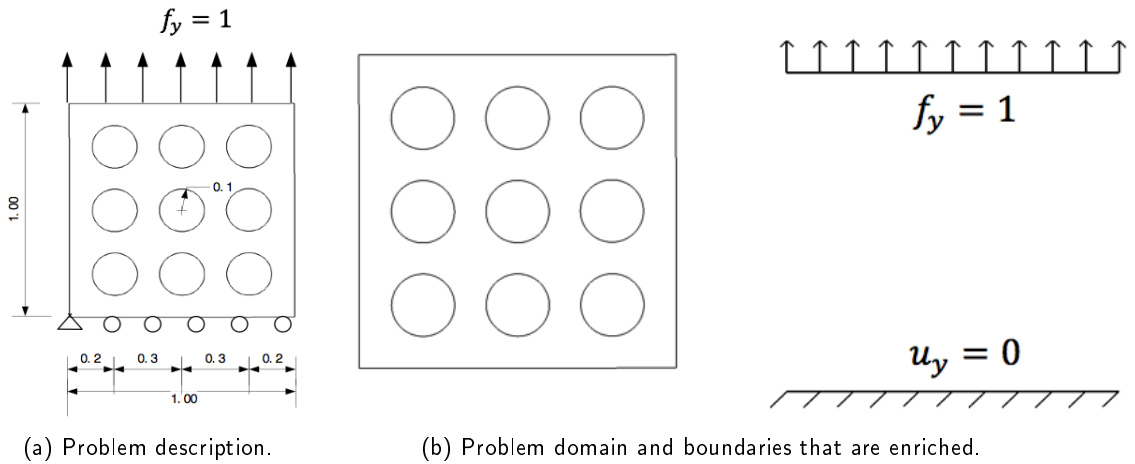


Figure 18: Example 2: Plate with multiple holes.

4.3 Curved T-structure

In this example, a curved T-shape under uniform compressive load on the top is analyzed. Fig. 19b shows the model geometry. The boundary of the geometry is not coincident with the edge of the background grid. Fig. 19c shows the T-geometry immersed in the NURBS background mesh. The signed algebraic level set that enables point classification is shown in Fig. 19d. The weight field constructed on the boundaries is shown in Fig. 19e. The background grid is 200×200 and the the blending region is twice the NURBS grid spacing as before. The Von mises stress generated through the analysis is shown in Fig. 19f. It is clear that even though the applied pressure is uniform, the sharp corner is a source of significant stress concentration.

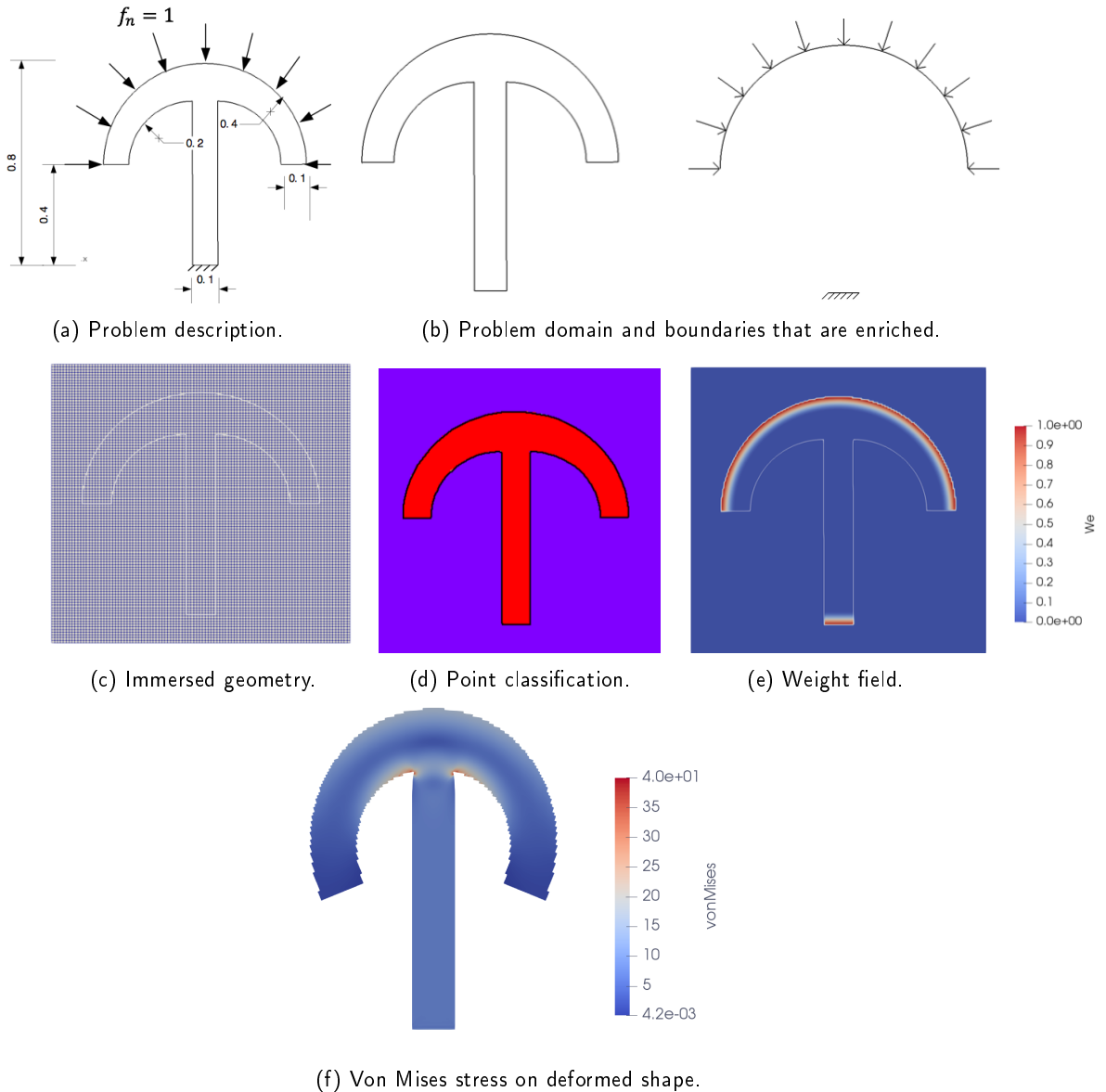


Figure 19: Example 3: Curved T-shape.

4.4 Loaded Wheel

The fourth example is that of a wheel under compression. The diameter of the wheel is 0.9 units and the applied pressure on top is 1. The length of the boundary on which the pressure is applied is 0.02 units. A region of the same size is fixed on the bottom of the geometry. The background mesh is again 200×200 and the blending region is again twice the grid size. As can be seen in Fig. 20f, the applied load is transferred to the hub by the nearest spokes. The deformation is consistent with the expectation that the wheel will be flattened under the load.

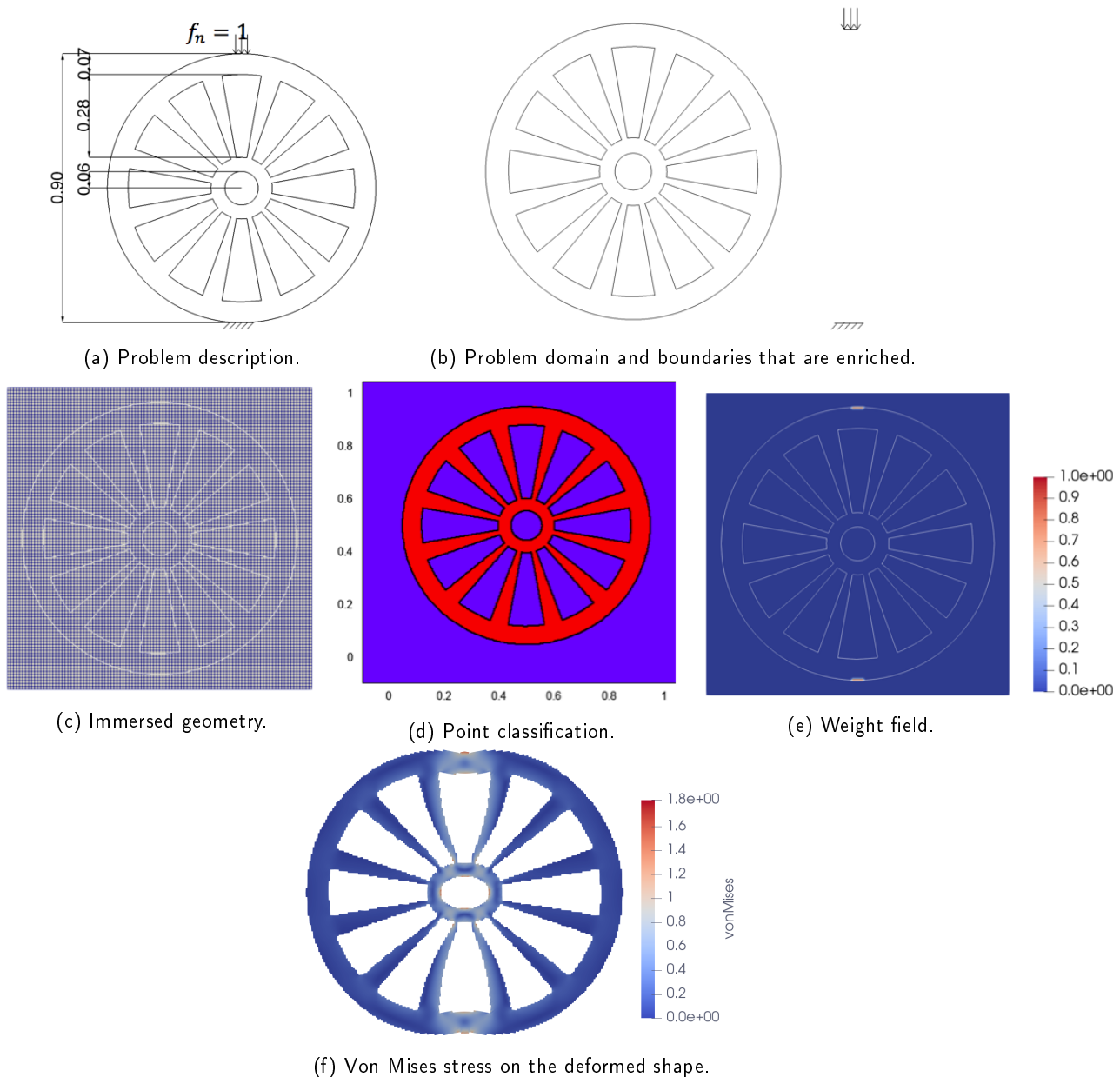


Figure 20: Example 4: Loaded Wheel.

5 Conclusions

In this paper, we described an approach to CAD-CAE integration that relies on immersing the CAD B-rep model into a regular NURBS analysis grid. Unlike the common weak imposition of boundary conditions in mesh free method, the approach described here enables direct application on the degree of freedom associated with the boundary.

The analysis methodology utilizes Enriched Isogeometric Analysis recently developed by the corresponding author and co-workers. EIGA utilizes extra degrees of freedom defined on the enriching boundary to blend fields with known behavior with those defined on the underlying analysis grid. This method avoids weak imposition of the boundary condition that is known to lead to poor numerical conditioning of the matrix system.

The use of algebraic level sets enables both construction of weight field and point classification. The former is necessary to capture the influence of boundaries on underlying domain, while the latter helps classify quadrature points as being inside the physical domain during analysis.

The proposed CAD-CAE integration approach eliminates mesh generation, retains a geometric representation of the boundaries that are exact to the CAD model, and enables exact to CAD point containment queries during analysis. The accuracy of the proposed method was demonstrated through both patch test as well as convergence analysis on a benchmark problem. In the patch test, decreasing the cell size leads to less error when using exponential weight function, while the cubic or quartic weight function yields solutions that are accurate to machine precision. In another benchmark test of a plate with hole under tension, the stress intensity factor was shown to converge to the theoretical solution with decreasing cell size. Several numerical examples were also provided to demonstrate the application and power of the developed method.

While the proposed approach is promising, further work is needed to describe algebraic level sets from a B-rep model consisting of multiple NURBS patches that are not mathematically closed, that is, from a B-rep model containing multiple patches that are not smooth across the patch boundaries. This need is important since commercial CAD systems often produce trimmed NURBS surfaces that are not smoothly joined (or stitched) at the trimming curves.

Yaxiong Chen, <http://orcid.org/0000-0002-2903-6723>

Chetan Jois, <http://orcid.org/0000-0001-6337-9482>

Ganesh Subbarayan, <http://orcid.org/0000-0003-0462-1130>

REFERENCES

- [1] Al Akhras, H.; Elguedj, T.; Gravouil, A.; Rochette, M.: Isogeometric analysis-suitable trivariate NURBS models from standard B-rep models. *Computer Methods in Applied Mechanics and Engineering*, 307, 256–274, 2016. <http://doi.org/10.1016/j.cma.2016.04.028>.
- [2] Babuška, I.: The finite element method with Lagrangian multipliers. *Numerische Mathematik*, 20(3), 179–192, 1973. <http://doi.org/10.1007/BF01436561>.
- [3] Belytschko, T.; Lu, Y.Y.; Gu, L.: Element-free Galerkin methods. *International Journal for Numerical Methods in Engineering*, 37(2), 229–256, 1994. <http://doi.org/10.1002/nme.1620370205>.
- [4] Biswas, A.; Shapiro, V.: Approximate distance fields with non-vanishing gradients. *Graphical Models*, 66(3), 133–159, 2004. <http://doi.org/10.1016/j.gmod.2004.01.003>.
- [5] Biswas, A.; Shapiro, V.: Heterogeneous material modeling with distance fields. *Computer Aided Geometric Design*, 21, 215–242, 2004. <http://doi.org/10.1016/j.cagd.2003.08.002>.
- [6] Cassale, M.: Ph.D. thesis.
- [7] Hughes, T.J.; Cottrell, J.A.; Bazilevs, Y.: Isogeometric analysis: CAD, finite elements, NURBS, exact geometry and mesh refinement. *Computer Methods in Applied Mechanics and Engineering*, 194(39-41), 4135–4195, 2005. <http://doi.org/10.1016/j.cma.2004.10.008>.
- [8] Juntunen, M.; Stenberg, R.: Nitsche's method for general boundary conditions. *Mathematics of Computation*, 78(267), 1353–1374, 2009. <http://doi.org/10.1090/S0025-5718-08-02183-2>.

- [9] Kagan, P.; Fischer, A.: Integrated mechanically based CAE systems using B-spline based finite elements. *Computer Aided Design*, 32, 2000.
- [10] Liu, W.K.; Jun, S.; Zhang, Y.F.: Reproducing kernel particle methods. *International Journal for Numerical Methods in Fluids*, 20(8-9), 1081–1106, 1995. <http://doi.org/10.1002/flid.1650200824>.
- [11] Liu, W.K.; Li, S.; Belytschko, T.: Moving least-square reproducing kernel methods (i) methodology and convergence. *Computer Methods in Applied Mechanics and Engineering*, 143(1-2), 113–154, 1997. [http://doi.org/10.1016/S0045-7825\(96\)01132-2](http://doi.org/10.1016/S0045-7825(96)01132-2).
- [12] Melenk, J.M.; Babuška, I.: The partition of unity finite element method: basic theory and applications. *Computer Methods in Applied Mechanics and Engineering*, 139(1-4), 289–314, 1996. [http://doi.org/10.1016/S0045-7825\(96\)01087-0](http://doi.org/10.1016/S0045-7825(96)01087-0).
- [13] Mortenson, M.E.: *Geometric Modeling*, 1997.
- [14] Natekar, D.; Zhang, X.; Subbarayan, G.: Constructive solid analysis: a hierarchical, geometry-based meshless analysis procedure for integrated design and analysis. *Computer-Aided Design*, 36(5), 473–486, 2004. [http://doi.org/10.1016/S0010-4485\(03\)00129-5](http://doi.org/10.1016/S0010-4485(03)00129-5).
- [15] Payne, B.A.; Toga, A.W.: Distance field manipulation of surface models. *IEEE Computer Graphics and Applications*, (1), 65–71, 1992. <http://doi.org/10.1109/38.135885>.
- [16] Peskin, C.S.: The immersed boundary method. *Acta Numerica*, 11, 479–517, 2002. <http://doi.org/10.1017/S0962492902000077>.
- [17] Piegl, L.; Tiller, W.: *The NURBS Book*. Springer Science & Business Media, 2012.
- [18] Renken, F.; Subbarayan, G.: NURBS based solution to inverse boundary problems in droplet shape prediction. *Computer Methods in Applied Mechanics and Engineering*, 190, 1391, 2000. [http://doi.org/10.1016/S0045-7825\(00\)00168-7](http://doi.org/10.1016/S0045-7825(00)00168-7).
- [19] Requicha, A.A.; Voelcker, H.B.: Boolean operations in solid modeling: Boundary evaluation and merging algorithms. *Proceedings of the IEEE*, 73(1), 30–44, 1985. <http://doi.org/10.1109/PROC.1985.13108>.
- [20] Rossignac, J.R.: Blist: A Boolean list formulation of CSG trees. Technical Report, Georgia Institute of Technology, 1999.
- [21] Ruess, M.; Schillinger, D.; Oezcan, A.I.; Rank, E.: Weak coupling for isogeometric analysis of non-matching and trimmed multi-patch geometries. *Computer Methods in Applied Mechanics and Engineering*, 269, 46–71, 2014. <http://doi.org/10.1016/j.cma.2013.10.009>.
- [22] Sederberg, T.W.: *Implicit and Parametric Curves and Surfaces for Computer Aided Geometric Design*. Ph.D. thesis, Purdue University, 1983.
- [23] Shapiro, V.: *Theory of R-functions and applications: A primer*. Technical Report, Cornell University, 1991.
- [24] Strouboulis, T.; Babuška, I.; Copps, K.: The design and analysis of the generalized finite element method. *Computer Methods in Applied Mechanics and Engineering*, 181(1-3), 43–69, 2000. [http://doi.org/10.1016/S0045-7825\(99\)00072-9](http://doi.org/10.1016/S0045-7825(99)00072-9).
- [25] Tambat, A.; Subbarayan, G.: Isogeometric enriched field approximations. *Computer Methods in Applied Mechanics and Engineering*, 245, 1–21, 2012. <http://doi.org/10.1016/j.cma.2012.06.006>.
- [26] Troyani, N.; Gomes, C.; Sterlacci, G.: Theoretical stress concentration factors for short rectangular plates with centered circular holes. *Journal of Mechanical Design*, 124(1), 126–128, 2002. <http://doi.org/10.1115/1.1496769>.
- [27] Upreti, K.; Song, T.; Tambat, A.; Subbarayan, G.: Algebraic distance estimations for enriched isogeometric analysis. *Computer Methods in Applied Mechanics and Engineering*, 280, 28–56, 2014. <http://doi.org/10.1016/j.cma.2014.07.012>.

- [28] Upreti, K.; Subbarayan, G.: Signed algebraic level sets on NURBS surfaces and implicit boolean compositions for isogeometric CAD–CAE integration. *Computer-Aided Design*, 82, 112–126, 2017. <http://doi.org/10.1016/j.cad.2016.09.006>.
- [29] Ventura, G.: An augmented lagrangian approach to essential boundary conditions in meshless methods. *International Journal for Numerical Methods in Engineering*, 53(4), 825–842, 2002. <http://doi.org/10.1002/nme.314>.
- [30] Wang, X.; Qian, X.: An optimization approach for constructing trivariate B-spline solids. *Computer-Aided Design*, 46, 179–191, 2014. <http://doi.org/10.1016/j.cad.2013.08.030>.
- [31] Zhang, Y.; Wang, W.; Hughes, T.J.: Solid T-spline construction from boundary representations for genus-zero geometry. *Computer Methods in Applied Mechanics and Engineering*, 249, 185–197, 2012. <http://doi.org/10.1016/j.cma.2012.01.014>.
- [32] Zhu, T.; Atluri, S.: A modified collocation method and a penalty formulation for enforcing the essential boundary conditions in the element free Galerkin method. *Computational Mechanics*, 21(3), 211–222, 1998. <http://doi.org/10.1007/s004660050296>.